Chapter 15
A Review of Multitemporal Synthetic Aperture Radar (SAR) for Crop Monitoring

Heather McNairn and Jiali Shang

Abstract Synthetic Aperture Radars (SARs) transmit and receive energy at microwave frequencies. The response recorded by these sensors is largely a function of the structure and dielectric properties of the target. The structure of a canopy is different among crops, and changes as crops grow. SARs respond very well to these structural differences and thus these sensors are able to accurately identify crop type and have proven sensitive to several crop biophysical parameters (Leaf Area Index, biomass, canopy height). Although optical sensors have traditionally been used for crop monitoring, advances in SAR applications research coupled with availability of SAR data at different frequencies and polarizations has raised the profile of these sensors for agricultural monitoring. And the "all weather" capability of SARs makes their use in operational activities of particular interest. Advancements in SAR applications development, continued improved access to data, and a push to transfer SAR research methods to monitoring agencies will lead to an increased role of SAR in monitoring agricultural production. This chapter reviews SAR research as it relates to crop type and acreage estimation, as well as determination of crop condition and crop bio-physical properties.

15.1 Requirements for Crop Monitoring

Balancing the supply of food with the demands from a growing global population is an ongoing challenge. To meet changing global food requirements, the UN Food and Agriculture Organization (FAO) estimated that food production must double in the next 40 years (www.un.org/News/Press/docs/2009/gaef3242.doc.htm). Quantifying food supply can be difficult as national, regional and global crop production fluctuates due to local land management decisions (what and where to seed) and meteorological conditions (principally precipitation and temperature). Anticipating production is further exacerbated when unforeseen disasters hit. Thus forecasting food supply necessitates on-going and frequent updates on acres seeded, yields

H. McNairn (✉) • J. Shang
Agriculture and Agri-Food Canada, Ottawa, ON, Canada
e-mail: heather.mcnairn@agr.gc.ca; jiali.shang@agr.gc.ca

Y. Ban (ed.), *Multitemporal Remote Sensing*, Remote Sensing
and Digital Image Processing 20, DOI 10.1007/978-3-319-47037-5_15

(bushels per acre) and meteorological parameters which impact crop growth. Crop production data can be gathered from a range of sources (for example, knowledge from extension workers, reports from farmers, climate data (Jayne and Rashid 2010)). Earth observing satellites also offer a source of data and as an example, will be used in initiatives such as the Group on Earth Observations Global Agricultural Monitoring (GEO-GLAM) to identify crop types and estimate acreages to monitor global food production (European Space Agency 2012).

Satellites suitable to map acreage and monitor crop growth condition are numerous. Sensors on these satellite platforms operate in both the electro-optical spectrum (400–2500 nm) and longer microwave wavelengths (1–100 cm). The configurations of these sensors also vary in terms of frequency of orbital repeat (and re-look), available swath and spatial resolution. At the global scale operational monitoring is for the most part, limited to coarser-resolution optical sensors such as the Moderate Resolution Imaging Spectroradiometer (MODIS) and the National Oceanic and Atmospheric Administration (NOAA) Advanced Very High Resolution Radiometer (AVHRR) (Becker-Reshef et al. 2010). These sensors are a source of daily data, yet their coarse spatial resolutions are less suitable for field-based production monitoring. When field-level monitoring is needed, higher resolution sensors are required.

15.2 Synthetic Aperture Radar (SAR) Responses to Crop Type and Condition

Optical sensors are well suited for mapping crop type and monitoring crop growth condition. At shorter wavelengths, the amount of solar energy absorbed, reflected and transmitted by vegetation is mainly driven by plant pigmentation as well as internal leaf structure and moisture. These chemical and physical properties (at the atom level) are crop type specific and are indicative of the growth stage and condition of the plant. At the other end of the electromagnetic spectrum, scattering of longer-wavelength microwaves is driven by larger scale structures (size, shape and orientation of leaves, stems and fruit) as well as the volume of water in the vegetation canopy (at the molecule level). Soil conditions (moisture and roughness) also effect microwave response. The significance of the effects of these soil conditions depends upon the crop type and growth stage, and the configuration of the microwave sensor. While optical wavelengths are more intuitively linked with crop condition, atmospheric conditions (for example presence of ozone, carbon dioxide, water, pollution) also cause absorption and scattering thus affecting spectral signals. As well, since these sensors rely on ambient energy imaging is limited to "daylight" hours.

Synthetic Aperture Radars (SARs), although currently not widely used for operational crop monitoring, provide a reliable source of data. These are active sensors generating their own source of energy, measuring the magnitude of transmitted energy scattered by the Earth back to the radar antenna. With their own source

of energy SARs can operate day or night and at these longer wavelengths are unaffected by the presence of cloud and haze. Using data from SARs for crop monitoring is not without challenge, primarily due to the confounding contributions of canopy moisture, crop structure and soil properties to the returned radar signal.

15.2.1 SAR Sensor Configurations

SAR sensors are defined by their operating frequency, incident angle and polarization. Incident angle can be defined by the angle (in degrees) between the radar beam and a line perpendicular to the Earth's surface. Each of these configurations affects the interaction of microwaves with the target in terms of backscatter intensity and scattering characteristics. Frequency (GHz or wavelength (cm)) and incident angle affect penetration depth of the transmitted microwave into the crop canopy. Depth of penetration increases with wavelength but decreases as angle increases. This depth affects which elements of the crop canopy interact with the microwave signal. Higher frequencies (i.e. X-Band with wavelengths of 2.4–3.75 cm) respond more to upper canopy structures while lower frequency (i.e. L-Band with wavelengths of 15–30 cm) microwaves penetrate further and generate more interaction with structures lower in the canopy. McNairn et al. (2009a) suggested that this differential penetration was the reason that crops were best identified when C-Band and L-Band data were integrated into a classifier; the higher frequency C-Band microwaves penetrated low biomass crops (wheat and hay-pasture) without significant interference from the soil, while L-Band waves penetrated further into larger biomass crops (corn and soybeans) allowing greater canopy interaction. Also important, to create scatter from a target element the target should be of equivalent size or larger than the wavelength of the transmitted wave. Otherwise attenuation of the radar signal will dominate.

Polarization is defined by the orientation of the electric field vector of the transmitted and received electromagnetic wave (Raney 1998). Polarization should be interpreted in the context of the structure of the target. The types of scattering from a target are identified as single bounce (surface), multiple (volume) or double-bounce. One source of scattering typically dominates, but depending on the complexity of the target secondary and tertiary sources of scattering can also be present. For well-developed crop canopies, vertical structures (stalks) can create double-bounce scattering, randomly oriented leaves, stems and fruit volume scattering, and large scatters (leaves, stems) oriented towards the sensor can result in single bounce scattering. Direct scattering from the soil, as well as double-bounce and multiple scattering events between the soil and canopy, may also contribute to the SAR response. The contribution from the soil will depend on penetration depth (determined by frequency, incident angle and canopy development).

Most SAR sensors transmit and receive microwaves in the horizontal (H) and/or vertical (V) linear polarizations. Early satellites transmitted and received microwaves in a single linear polarization (European Remote Sensing 1 and 2

(ERS-1/2) (VV), Japanese Earth Resources Satellite 1 (JERS-1) (HH) and RADARSAT-1 (HH)). Second-generation sensors (i.e. Advanced Synthetic Aperture Radar (ASAR)) were capable of transmitting and/or receiving in both linear polarizations, generating like (HH and/or VV) as well as cross (HV or VH) polarizations. A linear cross polarization response (HV or VH) results when the transmitted wave (i.e. H) is re-polarized to its orthogonal polarization (i.e. V). A strong HV or VH response is characteristic of targets where multiple scattering (at least two bounces) dominates (Raney 1998). Without multiple or double-bounce scattering events, HV or VH response will be low.

15.2.2 SAR Polarimetry

Polarimetric-capable satellites (i.e. the Advanced Land Observation Satellite (ALOS) Phased Array type L-band Synthetic Aperture Radar (PALSAR), RADARSAT-2 and TerraSAR-X) capture the complete characterization of the scattering field by recording all four mutually coherent channels (HH, VV, HV, VH), as well as retaining and processing the phase information between orthogonal polarizations. With phase retained, users can synthesize any wave orientation or ellipicity (providing linear, elliptical or circular polarizations) in addition to parameters that characterize target scattering. SARs can transmit completely polarized waves, but multiple scattering events will completely or partially de-polarize the wave. The degree of de-polarization (d) increases as multiple and volume scattering increases. With multiple scattering events phase becomes less predictable (more random) from point to point within the target. Degree of de-polarization varies by crop type and condition. Single bounce scattering (from smooth soil before crop emergence, for example) creates little de-polarization (Evans and Smith 1991), while thick vegetation canopies created diffuse scattering and almost completely un-polarized responses (d close to 0) (Groot et al. 1992). Pedestal height is one measure of degree of de-polarization with height increasing as multiple scattering increases. Hinds et al. (1993) discovered that the degree of polarization varied by crop type, growth stage and polarization. For the same crop type, degree of polarization varied through the growth cycle, decreasing as the crop canopy developed and increasing as the crop matured and dried out.

Cloude-Pottier (1997) and Freeman-Durden (1998) provided methods to decompose the polarimetric SAR signal within each resolution cell into characteristics of target scattering. Cloude-Pottier decomposes the signal into a set of eigenvectors (which characterize the scattering mechanism) and eigenvalues (which estimate the intensity of each mechanism) (Alberga et al. 2008). From the eigenvalues, entropy (H) and anisotropy (A) are calculated. H measures the degree of randomness of the scattering (from 0 to 1); values near zero are typical of single scatter targets while entropy increases in the presence of multiple scattering events as expected in a crop canopy. Anisotropy estimates the relative importance of the dominant scattering mechanism and the contribution from secondary and tertiary scattering mechanisms. Zero anisotropy indicates two mechanisms of approximately equal proportions; as

values approach 1 the second mechanism dominates the third (Lee and Pottier 2009). The average alpha ($\overline{\alpha}$) angle (0–90°) calculated by Cloude-Pottier identifies the dominant scattering source (Alberga et al. 2008). Single bounce scatters have alpha angles close to 0°; for crop canopies angles close to 45° (volume scattering) and nearing 90° (double-bounce) will be observed.

Freeman-Durden (1998), a three-component decomposition method, separates the total power of each SAR resolution cell into contributions from three scattering mechanisms – single bounce (surface), volume (multiple) and double bounce. This decomposition provides the magnitude of the contribution from each scattering mechanism.

15.2.3 Crop Characteristics Affecting SAR Response

SARs measure the intensity of energy scattered from targets back towards the radar antenna (recorded as backscatter in decibels (dB)). Properties of the target affect not only the intensity of backscatter, but also the scattering behavior. Scattering caused by natural targets can only occur when the radar waves encounter a dielectric discontinuity. Typically discontinuity is due to the presence of water which has a high dielectric constant (∼80) relative to air (∼1) (Dobson and Ulaby 1998). Backscatter is positively correlated with the dielectric constant of a target and thus typically, backscatter increases as water content increases. This relationship has been demonstrated repeatedly for soils, with higher backscatter recorded as soil moisture increases. However the relationship between canopy water content and SAR backscatter is more complex due to the sensitivity of SAR response to canopy structure. Findings have been mixed depending on the crop type, growth stage and SAR configuration. Studies have reported negative correlations with canopy water content for cereals (Hinds et al. 1993 using Ku-VV) and potatoes (McNairn et al. 2002 using C-HH). For canola, positive correlations with volume of canopy water have been reported by some (Hinds et al. 1993) while others reported no correlation (McNairn et al. 2002).

It is precisely because microwave scattering is sensitive to canopy structure that SARs can provide information on crop type and condition. When targets are physically oriented to the polarization of the incident wave, greater microwave interaction occurs. This is most pronounced for crops with vertical structures which align well with vertical (V) transmitted waves. Secondly the structure (stems, leaves, fruit) within the crop volume create ample opportunity for multiple scattering events which re-polarize and de-polarize the incident wave. Re-polarization creates higher HV or VH backscatter while de-polarization increases the un-polarized component of the scattered wave. Considering the scattering in the context of crop canopy structures, the linear cross polarization (HV or VH) has repeatedly proven to be the single best polarization for classification (Paris 1983; Brisco et al. 1991; Foody et al. 1994; McNairn et al. 2000, 2009a, b). Increases in classification accuracy can be achieved by including a second polarization into the classification. Because of the coupling of V-polarized waves with the vertical crop structure, an integration of

VV and VH (or HV) is preferred (McNairn et al. 2009a, b; Deschamps et al. 2012; McNairn and Shang 2014). Smaller incremental improvements are also reported with the inclusion of a third polarization (typically HH) (McNairn et al. 2000, 2009a; Hoekman and Vissers 2003).

Planting density and row direction (relative to the SAR look direction) can also impact SAR response. The intensity of scattering is generally higher when crop row direction is perpendicular rather than parallel to SAR look direction (Paris 1983). The cross polarization has the advantage of being insensitive to planting row direction (McNairn and Brisco 2004) and this, along with its sensitivity to canopy structure, make HV (or VH) an important polarization for crop monitoring. Wiseman et al. (2014) observed differences in C-Band backscatter and scattering responses among soybean fields due to differences in planting densities, even though all fields were at the same phenology stage.

15.3 Crop Classification to Support Acreage Estimation

15.3.1 Requirement for Multi-temporal SAR Data

Regardless of the sensor used, accurate crop identification requires that the energy recorded be unique to each crop type. Different crops can look "spectrally similar" at a given point in their growth cycle. For SARs, this confusion is due primarily to similarities in the crop structures. However, as crops move from one growth stage to the next, the development of leaves and fruit and the accumulation of biomass change the canopy structure, helping to differentiate one crop from another. The number of images required depends upon the crops present and the complexity of the cropping system (for example number of crops, consistency of planting practices, presence of inter-cropping and number of cropping seasons per year).

A key to successful crop classification is to understand which growth stages are best for crop separation and to identify which SAR configurations are best suited for crop classification. McNairn et al. (2009b) found that SAR response was very sensitive to changes in canopy structure during seed and fruit development, stages which occur later in the growing season. This study and a second study by Deschamps et al. (2012) recommended including a SAR image acquired during seed and reproductive phenology stages, at the point of peak biomass, in order to maximize classification accuracies.

15.3.2 Combining Multiple Frequencies for Crop Classification

Researchers have disagreed on recommendations for the optimal SAR frequency for crop discrimination. Discrepancies are most likely due to differences in crops

(and thus canopy structure and total canopy biomass) among the various studies. Some studies have reported that shorter Ku-, X- and C-Band wavelengths were very sensitive to canopy architecture and were better at separating crops (Bouman and Hoekman 1993; Brown et al. 1992; Paris 1986). Longer wavelengths penetrate deeper into the canopy and for low biomass crops this could introduce scattering from the soil. Yet for larger biomass crops these lower frequencies offer more opportunity for waves to interact with deeper canopy structures. Jia et al. (2012) favoured longer wavelengths at C-Band (ASAR) over X-Band (TerraSAR-X) for separating winter wheat from cotton. McNairn et al. (2009a) found that longer L-Band data (from ALOS PALSAR) was needed to accurately identify higher biomass crops (corn, soybean), although C-Band data was most suitable for separating lower biomass crops (wheat, hay-pasture).

Regardless of conclusions regarding the single best frequency, researchers agree on the advantages of integrating SAR acquired at multiple frequencies. Wooding (1992) clearly stated that discrimination of crops was best achieved by integrating SAR data acquired at more than one frequency, rather than combining two polarizations or two incidence angles. Using airborne and satellite SAR platforms researchers have determined that relative to single frequency data, higher crop classification accuracies are achieved using X- and C-Band (Thomson et al. 1990; Jia et al. 2012), C- and L-Band (Bouman and Uenk 1992; Dobson et al. 1996; Skriver 2012) X-, C- and L-Band (Brisco and Protz 1980; Guindon et al. 1984; Baghdadi et al. 2009), and C- and L- and P-Band (Chen et al. 1996; Ferrazzoli et al. 1997, 1999; Hill et al. 2005; Hoekman et al. 2011).

Engineering advances have meant that current SAR sensors can now provide data at multiple polarizations (in some cases fully polarimetric) and multiple incident angles. Studies have also used multi-frequency airborne or scatterometer sensors, or combined data from satellites operating at different frequencies, to demonstrate the importance of multiple frequencies for crop separation. Yet even with these multi-polarization and multi-frequency data, the temporal domain remains critical to successfully separate crop types (Skriver et al. 2011). Thus when multi-temporal data are available at multiple SAR configurations, crop classification is successful. As an example, McNairn and Shang (2014) report that when a multi-temporal C-Band data set with all linear polarizations (HH, VV, HV/VH) is available, high overall accuracies are achievable. Depending on the crop mix, accuracies of 85.5 % (more complex cropping system) to 90 % (simple mix of corn, soybeans, wheat, and pasture) are reached.

15.3.3 Full and Compact Polarimetry for Crop Classification

As described in Sect. 15.2.2 when a SAR sensor operates in a full polarimetric mode, the intensities of all four mutually coherent channels (HH, VV, HV, VH) are recorded as well as the phase information between orthogonal polarizations (also referred to as quadrature polarization (QP) sensors). Some improvement

in accuracies has been reported when decomposition parameters generated from these polarimetric data are used in a classification. McNairn et al. (2009a) used polarimetric L-Band data from ALOS PALSAR to demonstrate that overall accuracies improved by 4–7 % when decomposition parameters (from Cloude-Pottier, Freeman-Durden or Krogager) were used instead of the four linear intensity channels (HH, VV, VH/HV). Although all crops fell within the same class of scatterers, differences in the relative contributions of scattering mechanisms among the crops was observed and the authors attributed this to the improved classification.

These results were repeated when McNairn and Shang (2014) examined decompositions (Cloude-Pottier and Freeman-Durden) applied to C-Band RADARSAT-2 data. However increases in overall accuracies were smaller at this frequency. This research found that when overall accuracy using all linear polarizations is high (90 %), gains are minor (1–2 % when using the Cloude-Pottier entropy, alpha and anisotropy; 1–3 % when using the Freeman-Durden surface, volume and double-bounce scattering). Nevertheless, decomposition parameters will improve accuracies when the linear polarizations are unable to reach accuracies above 90 %.

In order to acquire the full scattering matrix, polarimetric sensors must double their Pulse Repetition Frequency (PRF) which immediately reduces the swath coverage by half (Charbonneau et al. 2010). Consequently, polarimetric acquisitions can be problematic if the intent is to use this mode for regional or national mapping. With compact polarimetry (CP) only one polarization is transmitted, and two orthogonal polarizations are received with the relative phase between the two received polarizations retained (Raney 2006). A CP SAR accesses the 2×2 covariance matrix of the backscattered field and thus contains less information than full polarimetric (QP) data (Charbonneau et al. 2010). However the main advantage of CP is that this mode does not force a reduction in swath. The RADARSAT-Constellation will implement a CP mode in a hybrid-polarity (CL) configuration where H and V will be transmitted simultaneously and 90° out of phase (circular polarization) and dual linearly polarizations will be received (Charbonneau et al. 2010).

To prepare to exploit this CP-CL mode for crop classification, full polarimetric RADARSAT-2 data have been used to simulate CP data. Results from the decompositions of the full polarimetric data (QP) and the Stokes vector parameters from CP have been compared. McNairn and Shang (2014) assessed QP decompositions and the four Stokes vector parameters from CP against the four linear intensity channels (HH, VV, VH, HV) for classification accuracy. The comparisons were carried out for three cropping systems. When the linear polarizations produced accurate (85–90 %) end of season classifications, the QP decompositions provided only small gains (1–2 % increase using Cloude-Pottier; 1–3 % increase using Freeman-Durden). With inputs from the Freeman-Durden decomposition classifications reached accuracies of 87–91 %. The Stokes vectors from CP produced similar results to the QP classifications. This confirmed early results reported in Charbonneau et al. (2010) for a simple cropping mix where late season results using the Stokes vectors were similar to QP decomposition results. In this case, using the Stokes vector parameters synthesized from four C-Band RADARSAT-2 images, end of season classification reached 91 % with individual crop classification accuracies ranging from 81 to

96 %. Both studies (McNairn and Shang 2014; Charbonneau et al. 2010) reported improvement in mid-season classifications using the Stokes vector parameters or QP decompositions, relative to results using the four linear polarizations. By mid-July classification accuracies for canola were 70 % (QP), 80 % for small grains (QP), 80 % for corn (QP or CP), 93 % for wheat (QP or CP) and 80 % for soybeans (CP).

CP is a relatively new concept in land applications and these results are considered preliminary. Although more research is needed, results to date indicate that both QP and CP hold promise for early, mid- and end-of-season crop classification.

15.3.4 Case Studies – The Successful Application of SAR for Crop Classification

Monitoring Rice Acreages Rice is a staple food for many providing between 30 and 70 % of the daily calories for half the world's population (Chen and McNairn 2006). In China, rice accounts for about 42 % of the nation's food production (Pei et al. 2011). Consequently, disruptions in rice production can seriously impact global food security. For this important commodity forecasting supply is critical.

Many studies have documented success in mapping rice paddies and monitoring rice growth using SAR. Backscatter increases significantly during a short period of vegetation growth, although large spatial variations in rice crop growth occur due to shifts in the crop calendar. Many studies have demonstrated sensitivity of multi-temporal C-Band backscatter to the phenology of rice growth, including Le Toan et al. (1997) who used ERS-1 (C-VV), Ribbes (1999) as well as Shao et al. (2001) who used RADARSAT-1 (C-HH), Chen et al. (2007) who used ASAR (HH and HV), Yang et al. (2008) who used ASAR (VV and HH) and Zhang et al. (2009) who used ALOS PALSAR. Classification accuracies of rice paddies have typically been reported well above 90 % (Shao et al. 2001; Li et al. 2003). Choudhury and Chakraborty (2006) used multi-temporal RADARSAT-1 ScanSAR data and a knowledge-based decision rule classifier to achieve 98 % accuracy. Chen and McNairn (2006) used multi-temporal RADARSAT-1 fine mode data to identify hectares (ha) of rice paddies in a region of the Philippines. A minimum mapping accuracy of 96 % was achieved. The authors then used C-HH backscatter from RADARSAT-1 to predict rice yield (kg/ha) to an accuracy of 94 %. Timing of rice planting was also mapped.

The legacy of C-Band sensors has meant a focus on this frequency although more recent research has evaluated space-borne X-Band for rice monitoring. In a study in southern China TerraSAR-X dual-polarized (VV, VH) data were used to map rice acreage, as well as to estimate changes in rice acreage between two years (2008 and 2009) (Pei et al. 2011). Using each individual TerraSAR-X image for each year, rice paddies were classified to a 95.6 % accuracy. Combining these 2 years of data, the change in acreages of rice was estimated to an overall accuracy of 99.0 % (Fig. 15.1). The study reported that almost 15 000 ha of rice was under cultivation

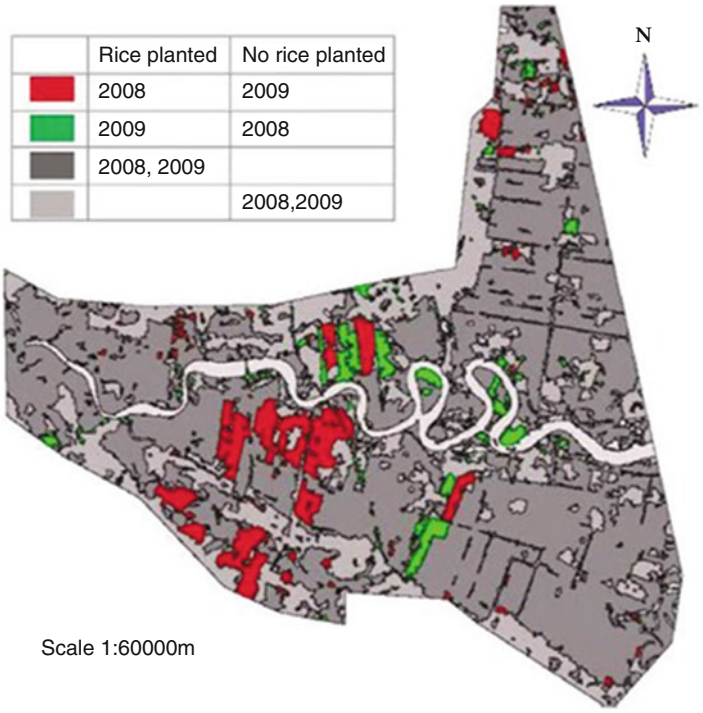

Fig. 15.1 Changes in acreages of late rice between the 2008 and 2009 seasons (Xuwen, China). Paddies planted in rice in 2008 but not 2009 are mapped in *red*; those planted in rice in 2009 but not 2008 are mapped in *green*. Land planted in rice both years appears in *dark grey*. Non-rice fields are identified in *light grey* (Taken from Pei et al. 2011)

in the Xuwen study site and that about 10 % of this land experienced change (rice to non-rice or non-rice to rice). Experts speculated that rice acreage change in this area was driven mainly by market demand as prices of other cash crops such as peanut and watermelon were high spurring some farmers to drain rice paddies to plant cash crops (Pei et al 2011). These annual fluctuations in rice production were deemed significant as they impact local and regional food security.

Operational End-of-Season Crop Mapping In one of the few examples of operational crop mapping with SAR data, Agriculture and Agri-Food Canada (AAFC) uses RADARSAT-2 and optical data to classify crops for all of Canada (Fig. 15.2) (Fisette et al. 2013). This inventory is delivered every year and supports policy and market development as well as program delivery. In 2011, Canadian Federal and Provincial governments paid out more than $420 M (CDN) to offset the impacts of climate related disasters, much of which was due to excessive soil moisture preventing farmers from seeding their fields. The AAFC crop inventory mapped the location of unseeded fields and was used to calculate the number of hectares affected. Acreage estimates from this satellite-derived map fell within 3 % of independent Provincial estimates (Fisette et al. 2013).

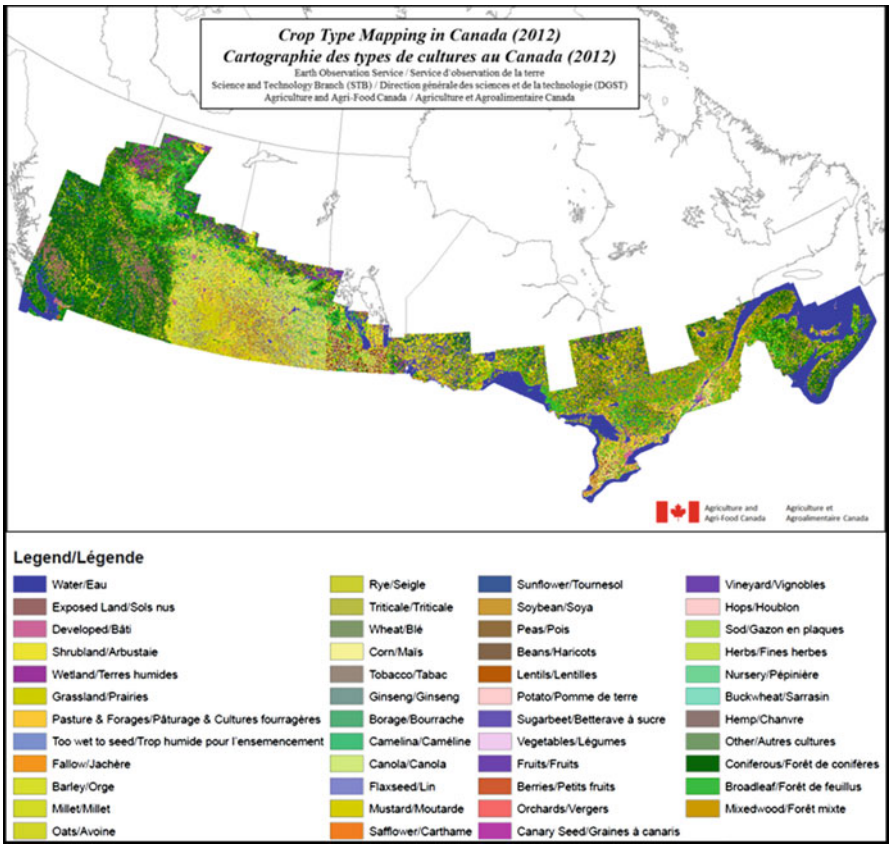

Fig. 15.2 The 2012 crop inventory for Canada. The map is created by classifying both optical and RADARSAT-2 satellite data. Image provided by Agriculture and Agri-Food Canada, Earth Observation Service

To produce this national crop map, data from optical satellites are integrated with C-Band data from RADARSAT-2. In 2013, the total number of scenes used included 1200 RADARSAT-2 scenes and 800 Landsat-8 images (Fisette et al. 2013). The project tasks dual-polarization (VV, VH) ScanSAR mode (300 km swath and 50 m resolution) over western Canada where fields are large and Wide mode (150 km swath and 30 m) over the rest of the country. Little is required to pre-process the SAR imagery other than ortho-rectification and speckle filtering. A Tasseled Cap transformation is applied to the Landsat data to reduce data processing. This is followed by semi-automated cloud and shadow masking.

Crops are classified using a supervised Decision Tree classifier, although a Random Forest classifier is being evaluated to improve processing time and accuracies (Fisette et al. 2013). Under agreements with crop insurance agencies AAFC accesses insurance data to train the classifier and validate the map product. For provinces where insurance data are unavailable, ground-truth information is collected by field crews. The inventory is able to consistently deliver a crop

inventory that meets the overall target accuracy of at least 85 % with a final product at a spatial resolution of 30 m (Fisette et al. 2013). Results from this operational project confirm the research leading to the implementation of the inventory (McNairn et al. 2009b); that integration of SAR can increase accuracies over the use of optical data alone. Here the addition of the RADARSAT-2 data has increased overall accuracies by up to 16 % (Fisette et al. 2013).

Early Season Crop Identification Forecasting in-season production means that crop acreage products must be delivered early in the season. Updates are required if multiple cropping occurs within a season or to improve the accuracy of early season acreage estimates. Considering the discussion in Sect. 15.3.1 where it was suggested that the highest accuracies are achieved when a classification uses SAR data collected at periods of peak biomass, delivery of early season products from this technology may be a challenge. Most studies in the literature have strived to maximize accuracies using all available data.

To evaluate the potential of SAR to deliver early season crop classification, McNairn et al. (2014a) used a supervised decision tree classifier with TerraSAR-X (VV, VH) and RADARSAT-2 (HH, VV, HV/VH). The cropping mix was relatively simple, with only three main crops present (corn, soybeans and hay-pasture). Either the C-Band or X-Band data were capable of delivering highly accurate maps of corn and soybeans at the end of the growing season. Accuracies far exceeded 90 % (Fig. 15.3). Of particular interest was the finding that with three early season TerraSAR-X images corn could be accurately identified by the end of June, a mere 6 weeks after planting and at a V6 vegetative growth stage (where the 6th leaf collar is visible). Identification this early in the season would assist in forecasting corn production. Soybeans required additional acquisitions given the variance in planting densities and planting dates in this region. In this case, accurate soybean classification required TerraSAR-X images until early August when seed development was beginning (R5 reproductive stage).

15.4 Monitoring Crop Condition with SAR

Production forecasting requires not only estimates of acreages planted (calculated from image classifications, for example) but also estimates of how productive crops appear to be. Different strategies have been adopted to estimate crop productivity from satellite data. A great deal of research has been undertaken to develop vegetation indices (primarily from optical sensors) and to use these as indicators of crop productivity (Becker-Reshef et al. 2010; Claverie et al. 2012; Gitelson 2004, 2011). Specifically, indices like the Normalized Difference Vegetation Index (NDVI) are tracked over the growing season and temporal changes in the index are compared to historical “normal” responses for the region. When indices are at or above “normals” crop production is expected to be on track. If these indices fall below historical norms, shortfalls in production might be expected. When coupled with knowledge of acreages, these provide estimates of total production.

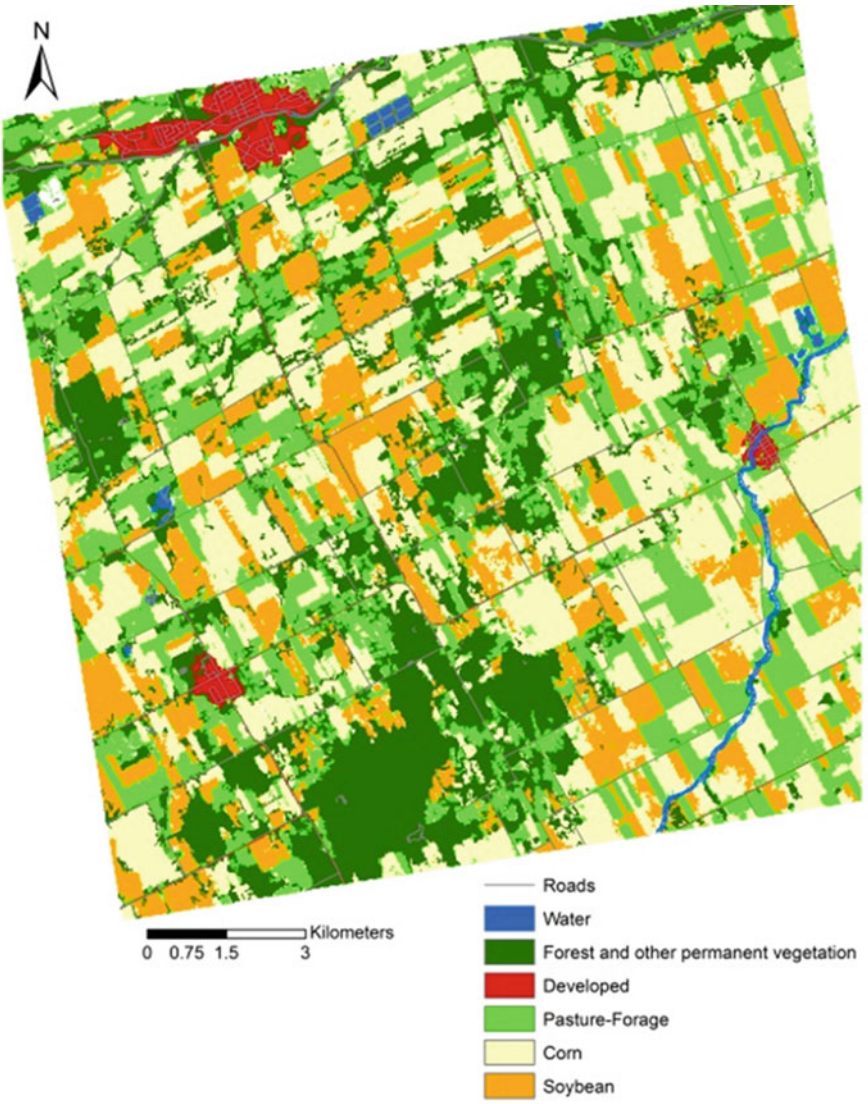

Fig. 15.3 An end-of-season classification map derived from TerraSAR-X (overall accuracy of 97.2 %) (Taken from McNairn et al. 2014a)

Alternatively, satellite response can be used to estimate crop properties which are chemically and biophysically related to crop yield. These properties include for example, biomass, height, leaf area, canopy water content, chorophyll and nitrogen content. The leaf area index (LAI) is linked to crop productivity and is a critical variable in many crop growth models. Optical remote sensing data have been used to estimate LAI and to calibrate these models (Baret and Guyot 1991; Chen and Cihlar 1996; Brown et al. 2000). Jégo et al. (2012) demonstrated that LAI estimates

from optical data, when assimilated into the Simulateur mulTIdiscplinaire pour les Cultures Standard (STICS) crop growth model, significantly improved yield and biomass prediction. However, knowledge of LAI variation during the entire crop cycle is essential for modelling crop growth and estimating crop yield (Clevers and van Leeuwen 1996). Interference by clouds often creates gaps in optical time series data. These gaps are problematic especially if they occur in the early season when biomass accumulation is greatest. With these challenges SAR data might be considered an option to fill these gaps, especially since microwaves respond to crop structure and thus the intensity and characteristics of scattering could be indicative of canopy biomass, height, LAI or water content.

Regardless of the approach taken, frequent multi-temporal acquisitions are needed to monitor crop condition and changes in these conditions through the entire cropping season. In addition to frequent temporal monitoring, estimates of these properties must be linked with both crop phenology and meteorological conditions, especially since vulnerability of crop growth detractants (disease, fungus) is dependent upon crop phenology (McNairn et al. 2014b).

15.4.1 Temporal Trends in SAR Response and Sensitivity of SAR to Crop Phenology

Although NDVI is perhaps the most widely recognized optically-based vegetation index, other indices can be linked with crop condition, and offer some advantages over NDVI. The Soil Adjusted Vegetation Index (SAVI) is of interest for multi-temporal monitoring of crop condition as this index is linked directly with LAI (Huete 1988 and Choudhury et al. 1994). SAVI has an advantage over other optical indices like NDVI since SAVI minimizes soil effects. When Freeman-Durden decomposition parameters (derived from RADARSAT-2) are compared with SAVI index values (derived from RapidEye), a similar temporal trend in response is observed (Fig. 15.4). Here volume (corn, canola and soybeans) and double-bounce (wheat) scattering derived from RADARSAT-2 increase after crop emergence during vegetative growth stages as crops accumulate leaf area and biomass. Peaks in scattering response are observed in mid-season, near coincident with when SAVI reaches its maximum. Both SAVI and scattering responses decline during the period of senescence, reaching a minimum at the point of harvest. This suggests that volume and double-bounce scattering are responsive to crop development over time, and that the use of these scattering parameters could be considered to temporally track crop condition in an approach similar to optical indices. Further research is needed, particularly since responses appear to be crop type specific.

A Radar Vegetation Index (RVI) was proposed by Kim and van Zyl (2009) for monitoring the vegetation growth using SAR. For natural targets RVI ranges

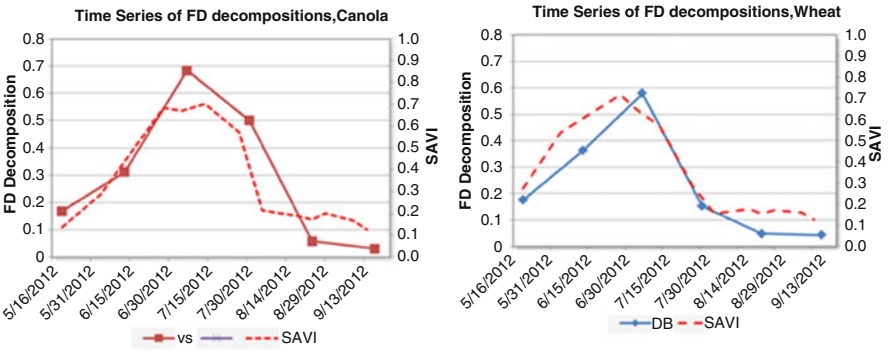

Fig. 15.4 Soil Adjusted Vegetation Index (*SAVI*) plotted with Freeman-Durden decompositions for canola (*VS* volume scattering) and wheat (*DS* double-bounce scattering) derived from C-Band RADARSAT-2. Responses are graphed from crop emergence (May) to senescence and harvest (August)

from 0 to 1 with values close to zero typical of smooth un-vegetated fields. As the vegetation canopy increases, scattering increases as does RVI. RVI is defined as:

$$RVI = \frac{8\sigma^{\circ}_{hv}}{\sigma^{\circ}_{hh} + 2\sigma^{\circ}_{hv} + \sigma^{\circ}_{vv}} \tag{15.1}$$

where σ^{o} is SAR intensity for each transmit (h or v) and receive (h or v) polarization. RVI derived from RADARSAT-2 is statistically correlated with plant height and plant area index (PAI) (Shang et al. 2013, 2014) and biomass (Wiseman et al. 2014). However, other SAR parameters that respond to volume scattering provide higher correlations. The RVI incorporates the linear co-polarizations which are less sensitive to volume scattering. In the case of HH, backscatter responses are largely created by single scattering events as would occur from direct soil interaction early in the growing season. The inclusion of these "less vegetation sensitive" polarizations in the RVI may explain these lower correlations.

Moran et al. (2012) confirmed that HV intensity at C-Band (from RADARSAT-2) is effective for temporally monitoring crop conditions. As well, these authors suggested that this cross-polarized backscatter could be used to track growth stages for grain (jointing and heading) and corn (leaf development and reproduction). Liu et al. (2013) studied the feasibility of monitoring crop growth based on a trend analysis of three basic scattering mechanisms using multi-year (2008–2010) RADARSAT-2 polarimetric data. In this case surface, double-bounce and volume scattering were generated using the Pauli decomposition. The temporal evaluation of the intensity of the scattering mechanisms generally tracked the measured LAI as well as phenology growth stage for wheat, corn and soybeans. Inoue et al. (2002) found that higher frequency X-Band backscatter was sensitive enough to detect thin

rice seedlings just after transplanting. Finally, Wiseman et al. (2014) reported that for spring wheat HV backscatter, volume scattering and pedestal height were able to detect when wheat entered the milking stage which could prove useful as an indicator for the timing of spring wheat harvest.

McNairn et al. (2014b) looked specifically at X- and C-Band responses for identifying the growth stage of canola. Canola is susceptible to a range of diseases which can impact yields. This crop is most vulnerable to fungal infection at flowering and insect infestation at the pod stage. If soil moisture is high at flowering, risk of fungal infection increases and yields can be reduced by as much as 50 %. This study found that X- and C-Band cross-polarization ratios (VV/VH) are high in the weeks following crop emergence due to the dominance of surface scattering from the soil. As canola leaves develop, volume scattering increases as does this ratio. A significant drop in this ratio (below 5 at X-Band and below 4 at C-Band) was observed when the canola flowered – a change in phenology of interest in monitoring for fungal infection. After flowering as the crop transitions to seed development, thick volumes of canola pods create significant multiple scattering increasing VH backscatter, with a further decline in the ratio observed. The decrease in the ratio at seed development was more pronounced at X-Band than C-Band, likely due to the small pods structures which are more closely aligned (in dimension) with X-Band wavelengths. At C-Band, the volume to surface ratio appeared to be more sensitive to pod development than the VV/VH ratio. Alpha angle from RADARSAT-2 was also interesting as the angle increased as scattering transitioned from surface to volume scattering.

15.4.2 Sensitivity of SAR to Crop Bio-physical Properties

15.4.2.1 Leaf Area Index

As far back as 1984, Ulaby et al. reported strong correlations between the LAI of corn and Ku-VV backscatter (up to an LAI of two, an R^2 of 0.9 was reported). Paris (1986) reported equally strong correlations at this high frequency (K-VV and K-HH) when examining LAI of corn. In the Ulaby study, only weak correlations were reported for wheat. Using lower frequency C-HH and C-VV backscatter, Ferrazzoli et al. (1992) also reported increases in backscatter with LAI. However as Ulaby et al. (1984) found, eventually the signal saturated becoming insensitive to further increases in LAI above a leaf area of 2–3. In a more recent study by Jiao et al. (2011) and using C-Band RADARSAT-2, sensitivity was lost above an LAI of three. Ulaby et al. (1984) explained that during the early stages of crop growth when LAI is less than 0.5, backscatter is dominated by soil moisture contributions. Leaf contributions dominate during periods of peak crop growth, but in the later stages just prior to harvest (LAI < 0.5), backscatter is dominated by soil and stalk contributions for corn, and by soil and head contributions from wheat. Jiao concurred and using the Water Cloud Model (WCM) found that at early growth stages (LAI less than one) soil moisture still had a significant contribution to scattering from corn and soybean

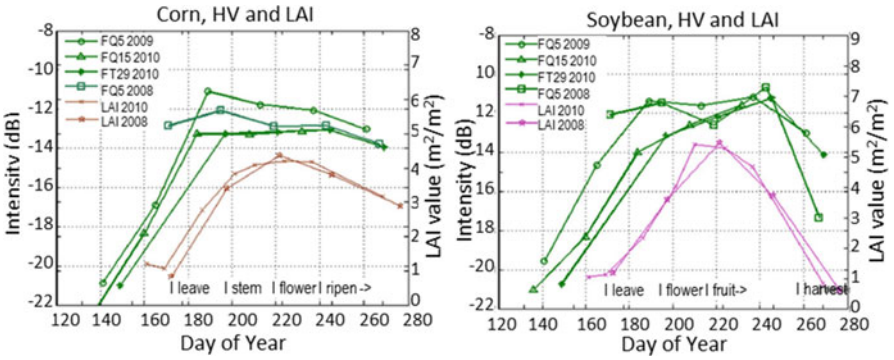

Fig. 15.5 Pauli volume scattering plotted with LAI for corn (*left*) and soybeans (*right*). Results are from 3 years of RADARSAT-2 data (2008, 2009 and 2010) collected in different fine quad (*FQ*) modes. Graphs taken from Liu et al. (2013)

fields. However, as the canopy developed and LAI increased to above one, scattering of C-Band microwaves was only minimally affected by soil moisture. After LAI reached three, 90 % of the scattering originated from the canopy.

Even though the evidence indicates that sensitivity is lost at higher LAI, SAR is sensitive to changes in LAI in the critical early growth stages. Additional studies have found strong correlations between SAR response and LAI for cotton (Maity et al. 2004 using C-Band), soybeans (Prasad 2011 using X-Band), corn and soybeans (Jiao et al. 2011 using C-Band) and wheat (McNairn et al. 2012 using C-Band). Liu et al. (2013) found that the RADARSAT-2 generated Pauli decomposition parameters generally tracked LAI development through the growing season (Fig. 15.5). Kim et al. (2013) monitored soybean growth over the season using data collected by an L-, C-, and X-band scatterometer. Although these results confirmed sensitivity to LAI, contrary to other studies, the authors reported that among the different frequencies and polarizations, L-band HH backscatter was most sensitive to growth changes and provided the highest correlation with LAI (as well as vegetation water content).

Jiao et al. (2011) and McNairn et al. (2012) correlated RADARSAT-2 SAR parameters to LAI for corn, soybeans and wheat. As previously observed, SAR parameters indicative of the intensity and characteristics of volume scattering (HV intensity, pedestal height, the Freeman-Durden volume scattering parameter and entropy) were strongly statistically correlated with LAI. Next, these authors parameterized with WCM using SAR responses, LAI and ancillary inputs of soil moisture. The WCM proved to adequately simulate SAR responses as the canopy developed and LAI increased, demonstrating the potential of polarimetric SAR data for monitoring indicators of crop productivity. The degree of model fit varied. For corn the fit (R^2) of LAI to these parameters ranged from 0.92 to 0.95 and for soybeans, 0.76–0.86. For wheat, entropy was selected with a goodness of fit statistic of 0.70. In McNairn et al. (2012) a Look Up Table was then used to invert the WCM and produce a map of LAI from RADARSAT-2 entropy.

15.4.2.2 Canopy Biomass

In addition to LAI, above ground dry biomass is a strong indicator of crop productivity (Liu et al. 2010) and thus monitoring dry biomass is of interest for yield forecasting. As might be expected, most researchers found HV intensity backscatter correlated with vegetation biomass (Paloscia 2002), although the sensitivity was crop type dependent. C-HV backscatter has proven correlated with dry biomass for corn, canola and soybeans (Ferrazzoli et al. 1999). However in an early study Ferrazzoli et al. (1997) reported strong correlations (R^2 of 0.75) between biomass and C-HV backscatter for smaller biomass crops like colza, wheat and alfalfa, but weak correlations (R^2 of 0.31) for corn, sunflower and sorghum, speculating that less weaker results were due to the signal saturation at C-Band. Mattia et al. (2003) used a simulated C-Band HH/VV channel to correlate response to wheat biomass, with an overall correlation of 0.87 reported.

Wiseman et al. (2014) closely examined correlations between C-Band response and dry biomass, and offered other explanations related to changes in crop phenology and thus canopy structure. In this 6 week study, responses of RADARSAT-2 to dry biomass were assessed for corn, canola, soybeans and wheat. SAR response increased more rapidly earlier in the season as biomass accumulation accelerated, leading to stronger correlations with non-linear (logarithmic) statistical models. For corn and canola, the strongest correlations with dry biomass were observed for entropy (R-values of 0.81 for corn and 0.84 for canola), suggesting that early in the season accumulations of biomass increased randomness in scattering within these canopies. For soybeans, the linear cross-polarized backscatter (HV) was most sensitive to increases in biomass (R-value of 0.81). For spring wheat, correlations were weak and these results were attributed to the late start of RADARSAT-2 acquisitions. Mid to late season, crop development was more focused on seed and fruit development and during these periods, a reduced rate of increase in SAR response was observed. It is at this point of crop development where SAR returns became more responsive to changes in growth stage rather than biomass (mostly leaf and stem) accumulation. This sensitivity to changes in structure due to phenology may partially explain reduced sensitivity of SAR to biomass from mid to late season. For canola C-HV backscatter reacted to flowering and ripening. For wheat HV backscatter, volume scattering and pedestal height changed as this crop entered its milking and dough stages.

15.4.2.3 Crop Height

Shang et al. (2013, 2014) illustrated that crop height for wheat is strongly correlated with both crop phenology and plant area index. Given this relationship, the authors explored sensitivity of RADARSAT-2 responses to wheat height and reported significant correlations (R^2) of 0.83 and 0.87 using both the HH and HV polarizations. The C-Band alpha angle gave even stronger correlations (R^2 of 0.93). This confirmed earlier results where McNairn et al. (2002) established that

crop height was significantly correlated with C-HH (RADARSAT-1) backscatter. In McNairn et al. (2002) height, biomass and LAI were used together to in a multi-variate statistical model to more fully characterize the crop canopy. With this multi-variate model as much as 85 % of the variance in C-HH backscatter was explained. Results were crop type dependent with the best RADARSAT-1 results from lower biomass wheat and potato crops. C-HH backscatter was insensitive to variations in corn growth. However using RADARSAT-2 C-HV backscatter, Shang et al. (2014) demonstrated good sensitivity to corn crop height and PAI, with R^2 values of 0.88 and 0.92 respectively. This sensitivity to crop height also explained variances in RADARSAT-2 responses among corn fields in a study completed by Wiseman et al. (2014).

15.5 Summary

A growing global population and a changing environment are placing increased pressure on the agriculture sector to continue to meet requirements of food supply. Early indications of imbalances in regional and global supplies can assist in managing these inequities to avoid crises in food security. Earth observing satellites provide one source of data to map acreages planted and crop growth, and to monitor changes in production over space and time. Although optical sensors have been used extensively for this purpose, poor atmospheric conditions can lead to gaps in data needed for ongoing monitoring. Synthetic Aperture Radar (SAR) sensors provide a reliable source of data, yet the interaction of active microwaves with crop canopies is complex.

Since the launch of the European Remote Sensing Satellite 1 (ERS-1) in 1991 and the Japanese Earth Resources Satellite 1 (JERS-1) in 1992 advances in SAR applications research have been significant. Today users have access to data from many more SAR satellites which operate at different frequencies (X-, C- and L-Band), varying incident angles and are either polarization-diverse or polarimetric-capable. SAR can accurately identifying crops, map crop acreages and identify acreage change. Yet as with optical sensors multi-temporal data is critical to successful classification. In addition higher accuracies are observed when multi-frequency SAR data are combined; research using quad-polarimetry or compact polarimetry SAR modes has proven that classification benefits from higher polarization diversity. Estimates of crop production also require data on crop growth. Here findings from scientists using different SAR sensors and cropping mixes have been consistent. Radar parameters which are responsive to canopy volume scattering (for example HV backscatter, entropy, volume scattering) are sensitive to canopy biophysical parameters including Leaf Area Index, biomass and height. These crop biophysical parameters can be used either directly or through assimilation into yield models to estimate crop productivity and when combined with crop maps, provide an estimate of total production.

The potential of SAR satellites to support national, regional and global crop monitoring is clear. Increased access to advanced SAR sensors, in conjunction with open data access, will foster wider use of this technology. This coming together of research and engineering sets the stage for a greater role for radar satellites in monitoring agricultural production and it is expected that as this technology accelerates, the contribution of SAR in creating knowledge on crop production will increase.

References

Alberga V, Satalino G, Staykova DK (2008) Comparison of polarimetric SAR observables in terms of classification performance. Int J Remote Sens 29:4129–4150

Baghdadi N, Boyer N, Todoroff P, El Hajj M, Begue A (2009) Potential of SAR sensors TerraSAR-X, ASAR/ENVISAT and PALSAR/ALOS for monitoring sugarcane crops on Reunion Island. Remote Sens Environ 113:1724–1738

Baret F, Guyot G (1991) Potentials and limits of vegetation indices for LAI and APAR assessment. Remote Sens Environ 35:161–173

Becker-Reshef I, Justice C, Sullivan M, Vermote E, Tucker C, Anyamba A, Small J, Pak E, Masuoka E, Schmaltz J, Hansen M, Pittman K, Birkett C, Williams D, Reynolds C, Doorn B (2010) Monitoring global croplands with coarse resolution Earth observations: the Global Agriculture Monitoring (GLAM) project. Remote Sens 2:1589–1609

Bouman BAM, Hoekman D (1993) Multi-temporal, multi-frequency radar measurements of agricultural crops during the Agriscatt-88 campaign in The Netherlands. Int J Remote Sens 14:1595–1614

Bouman BAM, Uenk D (1992) Crop classification possibilities with radar in ERS-1 and JER-1 configuration. Remote Sens Environ 40:1–13

Brisco B, Protz R (1980) Corn field identification accuracy using airborne radar imagery. Can J Remote Sens 6:15–24

Brisco B, Brown RJ, Gairns JG, Snider B (1991) Temporal radar observations of crops in western Canada. Can J Remote Sens 18:14–21

Brown RJ, Manore MJ, Poirier S (1992) Correlations between X-, C and L-band imagery within an agricultural environment. Int J Remote Sens 13:1645–1661

Brown L, Chen JM, Leblanc SG, Cihlar J (2000) A shortwave infrared modification to the simple ratio for LAI retrieval in boreal forests: an image and model analysis. Remote Sens Environ 71:16–25

Charbonneau FJ, Brisco B, Raney RK, McNairn H, Liu C, Vachon PW, Shang J, DeAbreu R, Champagne C, Merzouki M, Geldsetzer T, Trudel M (2010) Compact polarimetry overview and applications assessment. Can J Remote Sens 36:298–315

Chen JM, Cihlar J (1996) Retrieving leaf area index of boreal conifer forests using Landsat TM images. Remote Sens Environ 55:153–162

Chen C, McNairn H (2006) A neural network integrated approach for rice crop monitoring. Int J Remote Sens 27:1367–1393

Chen KS, Huang WP, Tsay DH, Amar F (1996) Classification of multifrequency polarimetric SAR imagery using a dynamic learning neural network. IEEE Trans Geosci Remote Sens 34: 814–820

Chen J, Lin H, Pei Z (2007) Application of ENVISAT ASAR data in mapping rice crop growth in southern China. IEEE Geosci Remote Sens Lett 4:431–435

Choudhury I, Chakraborty M (2006) SAR signature investigation of rice crop using RADARSAT data. Int J Remote Sens 27:519–534

Choudhury BJ, Ahmed NU, Idso SB, Reginato RJ, Daughtry CST (1994) Relations between evaporation coefficients and vegetation indices studied by model simulations. Remote Sens Environ 50:1–17

Claverie M, Demarez V, Duchemin B, Hagolle O, Ducrot D, Marais-Sicre C, Dejoux J-F, Huc M, Keravec P, Béziat P, Fieuzal R, Ceschia E, Dedieu G (2012) Maize and sunflower biomass estimation in southwest France using high spatial and temporal resolution remote sensing data. Remote Sens Environ 124:844–857

Clevers JGPW, van Leeuwen HJC (1996) Combined use of optical and microwave remote sensing data for crop growth monitoring. Remote Sens Environ 56:42–51

Cloude SR, Pottier E (1997) An entropy based classification scheme for land applications of polarimetric SAR. IEEE Trans Geosci Remote Sens 35:68–78

Deschamps B, McNairn H, Shang J, Jiao X (2012) Towards operational radar-only crop type classification: comparison of a traditional decision tree with a random forest classifier. Can J Remote Sens 38:60–68

Dobson MC, Ulaby FT (1998) Mapping soil moisture distribution with imaging radar. In: Henderson FM, Lewis AJ (eds) Principles and applications of imaging radar, manual of remote sensing, vol 2, 3rd edn. Wiley, New York, pp 407–433

Dobson MC, Pierce LE, Ulaby FT (1996) Knowledge-based land-cover classification using ERS-1/JERS-1 SAR composites. IEEE Trans Geosci Remote Sens 34:83–99

European Space Agency (2012) The Earth observation handbook: 2012 special edition for Rio + 20. European Space Agency, Noordwijk

Evans DL, Smith MO (1991) Separation of vegetation and rock signatures in thematic mapper and polarimetric SAR images. Remote Sens Environ 34:63–75

Ferrazzoli P, Paloscia S, Pampaloni P, Schiavon G, Solimini D, Coppo P (1992) Sensitivity of microwave measurements to vegetation biomass and soil moisture content: a case study. IEEE Trans Geosci Remote Sens 30:750–756

Ferrazzoli P, Paloscia S, Pampaloni P, Schiavon G, Sigismondi S, Solimini D (1997) The potential of multifrequency polarimetric SAR in assessing agricultural and arboreous biomass. IEEE Trans Geosci Remote Sens 35:5–17

Ferrazzoli P, Guerriero L, Schiavon G (1999) Experimental and model investigation on radar classification capability. IEEE Trans Geosci Remote Sens 37:960–968

Fisette T, Rollin P, Aly Z, Campbell L, Daneshfar B, Filyer P, Smith A, Davidson A, Shang J, Jarvis I (2013) AAFC annual crop inventory: status and challenges. The second international conference on agro-geoinformatics 2013, Fairfax, Virginia, 12–16 August 2013

Foody GM, McCulloch MB, Yates WB (1994) Crop classification from C-Band polarimetric radar data. Int J Remote Sens 15:2871–2885

Freeman A, Durden SL (1998) A three component scattering model for polarimetric SAR data. IEEE Trans Geosci Remote Sens 36:963–974

Gitelson AA (2004) Wide dynamic range vegetation index for remote quantification of biophysical characteristics of vegetation. J Plant Physiol 161:165–173

Gitelson AA (2011) Remote sensing estimation of crop biophysical characteristics at various scales. Hyperspectral remote sensing of vegetation. CRC Press, Boca Raton, pp 329–358

Groot JS, van den Broek AC, Freeman A (1992) An investigation of the potential of polarimetric SAR data for discrimination between agricultural crops. In: Proceedings of the MAESTRO-1/AGRISCATT: radar techniques for forestry and agricultural applications, Final Workshop, ESTEC, Noordwijk, The Netherlands, 6–7 March 1992

Guindon B, Teillet PM, Goodenough DG, Palimaka JJ, Sieber A (1984) Evaluation of the crop classification performance of X, L and C-band SAR imagery. Can J Remote Sens 10:4–16

Hill MJ, Ticehurst CJ, Lee J-S, Grunes MR, Donald GE, Henry D (2005) Integration of optical and radar classifications for mapping pasture type in western Australia. IEEE Trans Geosci Remote Sens 43:1665–1681

Hinds MR, Sofko GJ, Wacker AG, Koehler JA (1993) Ku-band polarization characteristics of crops and fallow, radar polarimetry. Proc SPIE 1748:47–58

Hoekman DH, Vissers AM (2003) A new polarimetric classification approach evaluated for agricultural crops. IEEE Trans Geosci Remote Sens 41:2881–2889

Hoekman DH, Vissers AM, Tran TN (2011) Unsupervised full-polarimetric SAR data segmentation as a tool for classification of agricultural areas. IEEE J Select Top Appl Earth Observ Remote Sens 4:402–411

Huete AR (1988) A Soil-Adjusted Vegetation Index (SAVI). Remote Sens Environ 25:295–309

Inoue Y, Kurosu T, Maeno H, Uratsuka S, Kozu T, Dabrowska-Zielinska K, Qi J (2002) Season-long daily measurements of multifrequency (Ka, Ku, X, C, and L) and full-polarization backscatter signatures over paddy rice field and their relationship with biological variables. Remote Sens Environ 2–3:194–204

Jayne TS, Rashid S (2010) The value of accurate crop production forecasts. Fourth African Agricultural Markets Program (AAMP) policy symposium, Lilongwe, Malawi, 6–10 September 2010

Jégo G, Pattey E, Liu J (2012) Using Leaf Area Index, retrieved from optical imagery, in the STICS crop model for predicting yield and biomass of field crops. Field Crop Res 131:63–74

Jia K, Li Q, Tian Y, Wu B, Zhang F, Meng J (2012) Crop classification using multi-configuration SAR data in the North China Plain. Int J Remote Sens 33:170–183

Jiao X, McNairn H, Shang J, Pattey E, Liu J, Champagne C (2011) The sensitivity of RADARSAT-2 polarimetric SAR data to corn and soybean leaf area index. Can J Remote Sens 37:69–81

Kim Y, van Zyl JJ (2009) A time-series approach to estimate soil moisture using polarimetric radar data. IEEE Trans Geosci Remote Sens 47:2519–2527

Kim Y, Jackson T, Bindlish R, Hoonyol L, Hong S (2013) Monitoring soybean growth using L-, C-, and X-band scatterometer data. Int J Remote Sens 34:4069–4082

Le Toan T, Ribbes F, Li-Fang W, Floury N, Kung-Hau D, Jin Au K, Fujita M, Kurosu T (1997) Rice crop mapping and monitoring using ERS-1 data based on experiment and modeling results. IEEE Trans Geosci Remote Sens 35:41–56

Lee JS, Pottier E (2009) Polarimetric radar imaging: from basics to applications. CRC Press, New York

Li Y, Liao Q, Li X, Liao S, Chi G, Peng S (2003) Towards an operational system for regional-scale rice yield estimation using a time-series of Radarsat ScanSAR images. Int J Remote Sens 24:4207–4220

Liu J, Pattey E, Miller JR, McNairn H, Smith A, Hu B (2010) Estimating crop stresses, aboveground dry biomass and yield of corn using multi-temporal optical data combined with a radiation use efficiency model. Remote Sens Environ 114:1167–1177

Liu C, Shang J, Vachon PW, McNairn H (2013) Multiyear crop monitoring using polarimetric RADARSAT-2 data. IEEE Trans Geosci Remote Sens 51:2227–2240

Maity S, Patnaik C, Panigraphy S (2004) Analysis of temporal backscattering of cotton crops using a semi-empirical model. IEEE Trans Geosci Remote Sens 42:577–587

Mattia F, Toan TL, Picard G, Posa FI, D'Alessio A, Notarnicola C, Gatti AM, Rinaldi M, Satalino G, Pasquariello G (2003) Multitemporal C-band radar measurements on wheat fields. IEEE Trans Geosci Remote Sens 41:1551–1558

McNairn H, Brisco B (2004) The application of C-band polarimetric SAR for agriculture: a review. Can J Remote Sens 30:525–542

McNairn H, Shang J (2014) Evaluation of C-band polarimetric synthetic aperture radar for crop classification. In: Principles and applications of PolInSAR, European Space Agency (ESTEC), Noordwijk, The Netherlands, in press

McNairn H, van der Sanden JJ, Brown RJ, Ellis J (2000) The potential of RADARSAT-2 for crop mapping and assessing crop condition. In: Proceedings of the 2nd international conference on geospatial information in agriculture and forestry, Lake Buena Vista, Florida, 10–12 January 2000

McNairn H, Ellis J, van der Sanden JJ, Hirose T, Brown RJ (2002) Providing crop information using RADARSAT-1 and satellite optical imagery. Int J Remote Sens 23:851–870

McNairn H, Shang J, Jiao X, Champagne C (2009a) The contribution of ALOS PALSAR multipolarization and polarimetric data to crop classification. IEEE Trans Geosci Remote Sens 47:3981–3992

McNairn H, Champagne C, Shang J, Holmstrom D, Reichert G (2009b) Integration of optical and Synthetic Aperture Radar (SAR) imagery for delivering operational annual crop inventories. ISPRS J Photogramm Remote Sens 64:434–449

McNairn H, Shang J, Jiao X, Deschamps B (2012) Establishing crop productivity using RADARSAT-2. International archives of the photogrammetry, remote sensing and spatial information sciences, Volume XXXIX-B8, 2012 XXII ISPRS Congress, Melbourne, Australia, 25 August–01 September 2012

McNairn H, Kross A, Lapen D, Caves R, Shang J (2014a) Early season monitoring of corn and soybeans with TerraSAR-X and RADARSAT-2. Int J Appl Earth Obs Geoinf 28:252–259

McNairn H, Wiseman G, Powers J, Merzouki A, Shang J (2014b) Assessment of disease risk in canola using multi-frequency SAR: preliminary results. In 10th European conference on synthetic aperture radar, Berlin, Germany, 2–6 June 2014

Moran MS, Moreno JF, Mateo MPC, de la Cruz DF, Montoro A (2012) A RADARSAT-2 quad-polarized time series for monitoring crop and soil conditions in Barrax. Spain IEEE Trans Geosci Remote Sens 50:1057–1070

Paloscia S (2002) A summary of experimental results to assess the contribution of SAR for mapping vegetation biomass and soil moisture. Can J Remote Sens 28:246–261

Paris JF (1983) Radar backscattering properties of corn and soybeans at frequencies of 1.6, 4.75, and 13.3 GHz. IEEE Trans Geosci Remote Sens 21:392–400

Paris JF (1986) The effect of leaf size on the microwave backscattering by corn. Remote Sens Environ 19:81–95

Pei Z, Zhang S, Guo L, McNairn H, Shang J, Jiao X (2011) Rice identification and change detection using TerraSAR-X data. Can J Remote Sens 37:151–156

Prasad R (2011) Estimation of kidney bean crop variables using ground-based scatterometer data at 9.89 GHz. Int J Remote Sens 32:31–48

Raney RK (1998) Radar fundamentals: technical perspective. In: Henderson FM, Lewis AJ (eds) Principles and applications of imaging radar, manual of remote sensing, vol 2, 3rd edn. Wiley, New York, pp 9–130

Raney RK (2006) Dual-polarized SAR and Stokes parameters. IEEE Geosci Remote Sens Lett 3:317–319

Ribbes F (1999) Rice field mapping and monitoring with RADARSAT data. Int J Remote Sens 20:745–765

Shang J, Jiao X, McNairn H, Kovacs J, Waters D, Ma B, Geng X (2013). Tracking crop phenological development of spring wheat using Synthetic Aperture Radar (SAR) in northern Ontario, Canada. The second international conference on agro-geoinformatics 2013, Fairfax, Virginia, 12–16 August 2013

Shang, J., Liu, J., Huffman, T., Ma, B., Zhao, T., McNairn, H., and Jiao, X. (2014). Using Earth observation to monitor corn growth in Ontario, Canada. In: Proceedings of the 68th Northeastern corn improvement conference, Ohio Agricultural Research and Development Centre, Wooster, Ohio, USA, 14–15 February, 2014

Shao Y, Fan X, Liu H, Xiao J, Ross S, Brisco B, Brown R, Staples G (2001) Rice monitoring and production estimation using multitemporal RADARSAT. Remote Sens Environ 76:310–325

Skriver H (2012) Crop classification by multitemporal C- and L-Band single- and dual-polarization and fully polarimetric SAR. IEEE Trans Geosci Remote Sens 50:2138–2149

Skriver H, Mattia F, Satalino G, Balenzano A, Pauwels VRN, Verhoest NEC, Davidson M (2011) Crop classification using short-revisit multitemporal SAR data. IEEE J Select Top Appl Earth Observ Remote Sens 4:423–432

Thomson KPB, Edwards G, Landry R, Jaton A, Cadieux SP, Gwyn QHJ (1990) SAR applications in agriculture: multiband correlation and segmentation. Can J Remote Sens 16:47–54

Ulaby FT, Allen CT, Eger G III, Kanemasu E (1984) Relating the microwave backscattering coefficient to leaf area index. Remote Sens Environ 14:113–133

Wiseman G, McNairn H, Homayouni S, Shang J (2014) RADARSAT-2 polarimetric SAR response to crop biomass for agricultural production monitoring. J Select Top Appl Earth Observ Remote Sens 7(11):4461–4471

Wooding MG (1992) Radar system configurations for crop and forest discrimination using AGRISCATT 8 data of the Feltwell Test Site. In: Proceedings of MAESTRO-1/AGRISCATT: Radar techniques for forestry and agricultural applications: Final Workshop, ESTEC, Noordwijk, The Netherlands, 6–7 March 1992

Yang S, Shuanghe S, Bingbai L, Le Toan T, Wei H (2008) Rice mapping and monitoring using ENVISAT ASAR data. IEEE Geosci Remote Sens Lett 5:108–112

Zhang Y, Wang C, Wu J, Qi J, Salas WA (2009) Mapping paddy rice with multitemporal ALOS/PALSAR imagery in southeast China. Int J Remote Sens 30:6301–6315